PHYSICAL REVIEW B **73**, 113101 (2006)

Electron momentum density and the Fermi surface of β-PdH$_{0.84}$ by Compton scattering

S. Mizusaki,* T. Miyatake, N. Sato, I. Yamamoto, and M. Yamaguchi
Department of Physics, Yokohama National University, Tokiwadai, Hodogaya-ku, Yokohama 240-8501, Japan

M. Itou and Y. Sakurai
Japan Synchrotron Radiation Research Institute, SPring-8,1-1-1 Kouto, Sayo, Hyogo 678-5198, Japan

(Received 16 August 2005; revised manuscript received 18 January 2006; published 6 March 2006)

The geometry of the Fermi surface of β-PdH$_{0.84}$ has been determined by the synchrotron-based Compton scattering experiment with 115 keV x rays. The Fermi surface is mapped out from the electron momentum density which is three-dimensionally reconstructed from 12 directional Compton profiles. It is found that the Fermi surface is a deformed electron sphere with a neck along the [111] direction like a noble metal. The Fermi momenta are 0.63 ± 0.02 atomic units in the [100] direction and 0.65 ± 0.16 atomic units in the [110] direction, and the neck radius is 0.18 ± 0.03 atomic units around the [111] direction. This result agrees satisfactorily with that of first-principles band structure calculations within the effective experimental momentum resolution.

DOI: 10.1103/PhysRevB.73.113101 PACS number(s): 71.18.+y, 71.20.Be, 71.20.Ps

The palladium-hydrogen system is an excellent prototype for investigating the hydrogen-induced changes in the physical properties of transition metals from the quantum mechanical point of view. The strong paramagnetism in Pd disappears in the β-PdH$_x$ ($x>0.6$), and the normal conducting state changes to the superconducting one in the β-PdH$_x$ ($x>0.8$) with an inverse hydrogen-isotope effect on its critical temperature.[1] These facts imply that hydrogen absorption profoundly influences the band structure and the Fermi surface (FS) of fcc Pd.

Theoretically, previous band structure calculations[2–8] for stoichiometric PdH or non-stoichiometric PdH$_x$ ($x<1$) have predicted that a metal-hydrogen bonding band is formed below the Pd d band and the position of the Fermi energy is raised from the d band to the so-called s,p bands. As a consequence, the FS is drastically changed to a deformed sphere with a neck along the [111] direction.[7,8]

Experimentally, the Pd hydrides have been investigated by several photoemission and photoabsorption spectroscopies.[9–13] These experiments have verified the general adequateness of calculated density of states in the electron energy aspect. In the electron momentum aspect, however, no experiments have yet obtained the FS of PdH$_x$ although a positron annihilation experiment has yielded fragmentarily the Fermi momenta p_{F} in PdH$_{0.72}$,[14] and a de Haas–van Alphen experiment has measured the extremal area of the FS cross-section in very dilute hydride PdH$_{0.01}$.[15,16] In general, these experimental methods are difficult to apply to metal hydrides with large hydrogen concentrations because of inevitable inclusion of crystal imperfections and instability of the hydride phases.

Recently, direct observations of the three-dimensional (3D) electron momentum density (EMD) have been developed with the synchrotron-based, high-resolution Compton scattering technique.[17–24] From a Compton scattering experiment, one obtains the so-called Compton profile (CP), $J(p_z)$, which is directly related to the ground-state EMD, $\rho(\mathbf{p})$, by

$$J(p_z)=\int\int \rho(\mathbf{p})dp_x dp_y, \tag{1}$$

where p_z is taken along the x-ray scattering vector.[25] Within an independent particle model, the EMD is expressed in terms of the electron wave function ψ_j,

$$\rho(\mathbf{p})=(2\pi)^{-3}\Sigma_j\left|\int \psi_j(\mathbf{r})\exp(-i\mathbf{p}\cdot\mathbf{r})d\mathbf{r}\right|^2, \tag{2}$$

where the summation in Eq. (2) extends over all occupied states. The 3D-EMD is reconstructed from a set of Cps measured along different crystallographic directions. The experimental FS is extracted by plotting extrema in the first derivatives of the EMD.[26]

Compton scattering is a unique technique to investigate metal hydrides because it is insensitive to crystal imperfections and allows an experiment under any gas atmosphere at any temperature.[27] In this paper, we present the FS of β-PdH$_{0.84}$ determined by the high-resolution Compton scattering method and discuss the geometry of the FS by comparing with that predicted by first-principles calculations.

A single-crystal β-PdH$_x$ was prepared by reacting a single crystal of Pd with hydrogen as described in the previous paper.[27] The Pd crystal is a cylinder with a diameter of 5 mm and a length of 5 mm, and its purity is 99.99%. The hydrogen composition was determined to be $x=0.84$ from the weight increase after the reaction. This hydrogen composition was confirmed to be unchanged after the experiment.

The Compton scattering experiment was carried out with the high-resolution Compton scattering spectrometer at the BL08W beamline of SPring-8. The energy of the incident x rays was 115 keV and the scattering angle was 165°. The sample was placed under 0.1 MPa helium gas atmosphere at room temperature to stabilize the hydride phase. Twelve Compton profiles were measured along different crystallographic directions. The accumulated count at the Compton peak is approximately 2×10^5 for each profile. The overall momentum resolution was 0.15 atomic units (a.u.) in the full

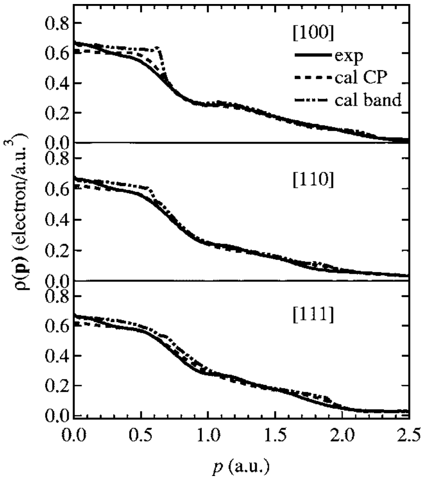

FIG. 1. Experimental electron momentum density (EMD), $\rho(\mathbf{p})_{exp}$, of β-$\mathrm{PdH}_{0.84}$ (solid lines) and calculated EMDs, $\rho(\mathbf{p})_{cal}^{CPS}$ (broken lines) and $\rho(\mathbf{p})_{cal}^{band}$ (dashed-and-dotted lines), of PdH along the highly symmetrical directions. $\rho(\mathbf{p})_{cal}^{CPS}$ is reconstructed from the calculated Cps in the same procedure to the data processing of the present experimental data, where the Cps are convoluted with the experimental resolution function. $\rho(\mathbf{p})_{cal}^{band}$ is directly obtained from the band structure calculated by the computational code (Ref. 27) without convolution with the experimental resolution function.

width at half maximum. The detail of the data analysis was described in the previous paper.[27]

The experimenral 3D-EMD, $\rho(\mathbf{p})_{exp}$, was reconstructed using the direct Fourier method. The reader is referred to Tanaka *et al.*[19] for the details of the method. In the reconstruction, the relationship between the reciprocal form factor, $B(\mathbf{r})$ and $\rho(\mathbf{p})$ is used,

$$B(\mathbf{r}) = \int \rho(\mathbf{p})\exp(-i\mathbf{pr})d\mathbf{p}. \tag{3}$$

The form factor, $B(\mathbf{r})$, along a direction in real space parallel to p_z can be obtained by a one-dimensional Fourier transform of $J(p_z)$ along the same direction,

$$B(0,0,z) = \int J(p_z)\exp(-ip_z z)dp_z. \tag{4}$$

When $J(p_z)$'s are measured along different crystallographic directions, $B(\mathbf{r})$'s can be obtained on the lines along the corresponding directions. Interpolation using the obtained $B(\mathbf{r})$'s gives interpolated values of $B(\mathbf{r})$ throughout the $\mathbf{r}$. Once $B(\mathbf{r})$ is known, $\rho(\mathbf{p})$ can be evaluated by the back Fourier transformation. This direct Fourier transform method was applied by Suzuki *et al.* to two-dimensional positron annihilation angular correlation data.[28] Later, the method was employed to reconstruct the 3D-EMD from $J(p_z)$.[17–24]

The error propagation in the reconstruction method was calculated using the same program developed by Tanaka *et al.*[19] It is found that the largest error of reconstructed $\rho(\mathbf{p})$ is 4.2% at $p=0$.

The band structure of stoichiometric PdH was calculated by the full-potential linearized augmented plane-wave method within the local density approximation (LDA-FLAPW) using the same computing code as the previous work.[27] We derived the theoretical EMD and Fermi surface via two routes. One is the direct route from the obtained band structure, termed the directly calculated EMD, $\rho(\mathbf{p})_{cal}^{band}$, and Fermi surface, FS_{cal}^{band}. $\rho(\mathbf{p})_{cal}^{band}$ is not convoluted with the experimental resolution function. The other is the indirect route that follows the data-processing procedure for the present experimental data: First, 12 Cps along the same directions as the experiment were calculated from the calculated wave functions, and then the theoretical 3D-EMD was reconstructed from the Cps. The Cps are convoluted with the experimental resolution of 0.15 a.u. The FS was determined by the same method as used in the experiment. They are termed the indirectly calculated EMD, $\rho(\mathbf{p})_{cal}^{CPS}$, and Fermi surface, FS_{cal}^{CPS}. It should be noted that $\rho(\mathbf{p})_{cal}^{CPS}$ and FS_{cal}^{CPS} include errors due to the experimental resolution, the reconstruction procedure, and the method to determine the Fermi momentum, while $\rho(\mathbf{p})_{cal}^{band}$ and FS_{cal}^{band} do not include them.

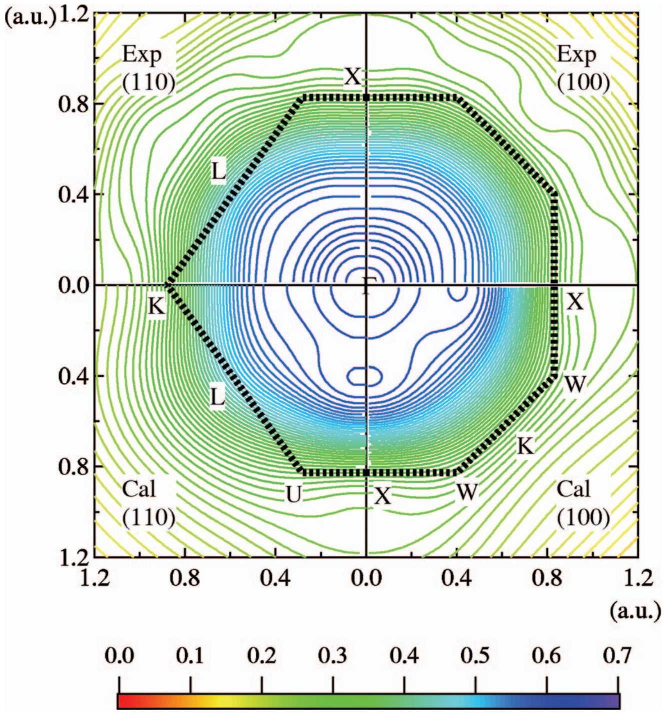

FIG. 2. (Color) Contour maps of the experimental and calculated EMDs, $\rho(\mathbf{p})_{exp}$ and $\rho(\mathbf{p})_{cal}^{CPS}$, on the (110) plane (left side) and the (100) plane (right side). The upper maps are the experimental $\rho(\mathbf{p})_{exp}$ of $\mathrm{PdH}_{0.84}$ and the lower ones are the calculated $\rho(\mathbf{p})_{cal}^{CPS}$ of PdH. The $\rho(\mathbf{p})_{cal}^{CPS}$ was reconstructed from 12 calculated Compton profiles, which are convoluted with the experimental resolution function, following the same procedure to the present experiment. The broken line is the first Brillouin zone boundary. The contour interval is 0.01 electron/a.u.^{3} in every map.

Figure 1 compares the experimental $\rho(\mathbf{p})_{exp}$ with the calculated $\rho(\mathbf{p})_{cal}^{CPS}$ and $\rho(\mathbf{p})_{cal}^{band}$ along the highly symmetrical directions. It is considered that there is no meaningful difference in the hydrogen composition between the experiment and the calculations, taking account of the experimental resolution.

Figure 2 illustrates the contour maps of the experimental and calculated EMDs, $\rho(\mathbf{p})_{exp}$ and $\rho(\mathbf{p})_{cal}^{CPS}$, on the (100) and

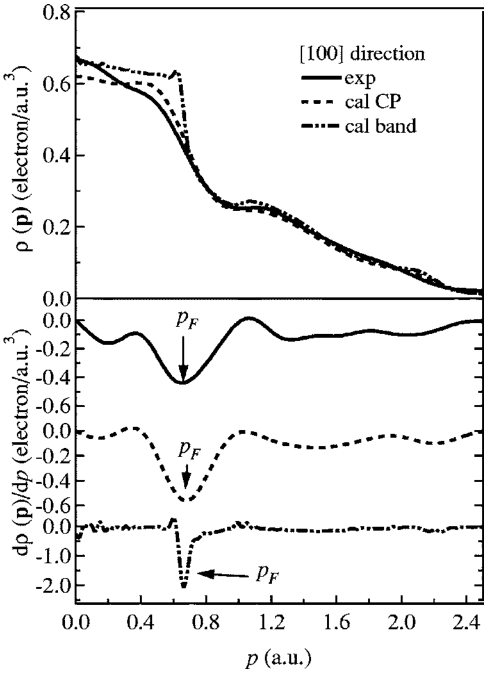

FIG. 3. First derivatives of the EMDs, $\mathrm{d}\rho(\mathbf{p})/\mathrm{d}p$, in the [100] direction for the experimental $\rho(\mathbf{p})_{exp}$ of $\mathrm{PdH}_{0.84}$ (solid lines) and the calculated $\rho(\mathbf{p})_{cal}^{CPS}$ (dashed-and-dotted lines) and $\rho(\mathbf{p})_{cal}^{band}$ (dotted lines).$\rho(\mathbf{p})_{cal}^{CPS}$ is reconstructed from the calculated Cps in the same procedure as the data processing of the present experimental data, where the Cps are convoluted with the experimental resolution function. $\rho(\mathbf{p})_{cal}^{band}$ is directly obtained from the band structure calculated by the computational code (Ref. 27) without convolution with the experimental resolution function. The Fermi momentum (p_{F}) is given as its extremum.

(110) planes to make clearer their anisotropies. The contour lines are deformed circles and bulge to the [111] direction (Γ-L) in both the experiment and the calculation. The calculated $\rho(\mathbf{p})_{cal}^{CPS}$ reproduces the experimental $\rho(\mathbf{p})_{exp}$ well.

Figure 3 explains the method to determine the position of p_{F} as the extremum in the first derivatives of the EMD along the [100] direction. The experimental p_F is pointed to be 0.63, which is inside of the first Brillouin zone (BZ) boundary at 0.83 a.u. along the [100] direction. When the calculated Cps are broadened to reflect experimental resolution and then the EMD is reconstructed from the broadened Cps, the shape in the first derivative carves becomes dull. However, the difference in the extremum between $\rho(\mathbf{p})_{cal}^{CPS}$ and $\rho(\mathbf{p})_{cal}^{band}$ is 0.02 a.u., and that of $\rho(\mathbf{p})_{cal}^{CPS}$ (0.68 a.u.) is in good agreement with the experiment. This fact shows that the p_{F} positions determined by the present method are not largely disturbed.

Mapping the Fermi momenta, we obtained the experimental FS (closed circles) on the (100) and (110) planes as shown in Fig. 4. In the [110] direction, the p_F is 0.65±0.16 a.u. inside of the first BZ boundary at 0.89 a.u. The FS is nearly circular on the (100) plane. In contrast to this, it touches the BZ boundary and forms a neck with a radius of 0.18±0.03 a.u. along the [111] direction on the (110) plane. This figure also plots the calculated FS_{cal}^{CPS} (solid lines) and FS_{cal}^{band} (open circles). The directly calculated FS_{cal}^{band} agrees well with that calculated by Gupta and Freeman.[7] The positron annihilation experiment by Hasegawa[14] yielded the p_{F} at three points (squares), which only agrees with the present result at the neck along the [111] directions.

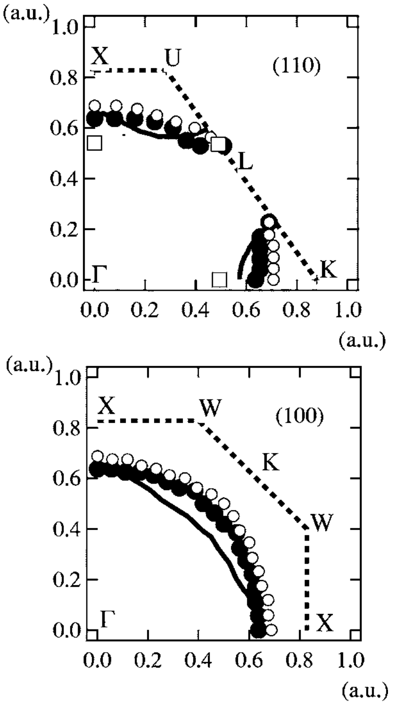

FIG. 4. Cross sections of the Fermi surface (FS) on the (110) plane (upper figure) and the (100) plane (lower figure). The closed circles are the experimental FS of $\mathrm{PdH}_{0.84}$. The open circles and the solid lines are the calculated FSs, FS_{cal}^{CPS}, and FS_{cal}^{band}, of PdH, respectively: FS_{cal}^{CPS} is determined from the reconstructed electron momentum density, $\rho(\mathbf{p})_{cal}^{CP}$ and FS_{cal}^{band} are directly obtained from the band structure calculated by the computational code (Ref. 27). The squares are the result of the positron annihilation experiment for $\mathrm{PdH}_{0.74}$ (Ref. 14). The broken lines are the first Brillouin zone boundary.

The difference δp_{F} between FS_{cal}^{CP} and FS_{cal}^{band} gives an estimated range of error in determining the FS with this method. In this paper, the value of δp_{F} is used as the error bar for the experimental Fermi momentum. The difference in the size of the neck between FS_{cal}^{CP} and FS_{cal}^{band} is also used as the error for the experimental value. The degree of the difference depends on the direction, varying from $\delta p_{\mathrm{F}}=0.02$ a.u. in the [100] direction to $\delta p_{\mathrm{F}}=0.16$ a.u. in the [110] direction. We have carefully examined the calculated EMD and have found that the size of the FS discontinuity along the [110] direction is smaller than those along other directions. This small discontinuity and the contribution of the occupied bands, both shift the extremum toward high momenta in the first derivatives.

Finally, Fig. 5 illustrates the isosurface on the occupation number density at a level of 0.60 electron/a.u.^{3} fixed by the momentum $p_{\mathrm{F}}=0.65$ a.u. The occupation number density is obtained by folding back the experimental EMD into the first BZ using the Lock-Crisp-West procedure.[29] This clearly shows that the electron surface is extended to the [111] direction in the first BZ and connected to the next zone with the neck. The FS of β-PdH$_{0.84}$ is geometrically quite similar to that of fcc Ag metal. It is reasonable because PdH has a hypothetical electron configuration of $4d^{10}5s^1$ similar to Ag. The neck radius of the β-PdH$_{0.84}$ is about two times larger than that of fcc Ag.[30] This shows that the Fermi level of β-PdH$_{0.84}$ is closer to the top of the d bands than that of fcc Ag metal and the wave functions at the Fermi level have larger d character.

In summary, we have determined the Fermi surface of β-PdH$_{0.84}$ on the (100) and the (110) planes via the electron momentum density obtained from the high-resolution Compton scattering experiment. The Fermi surface is a deformed electron sphere with a neck along the [111] direction.

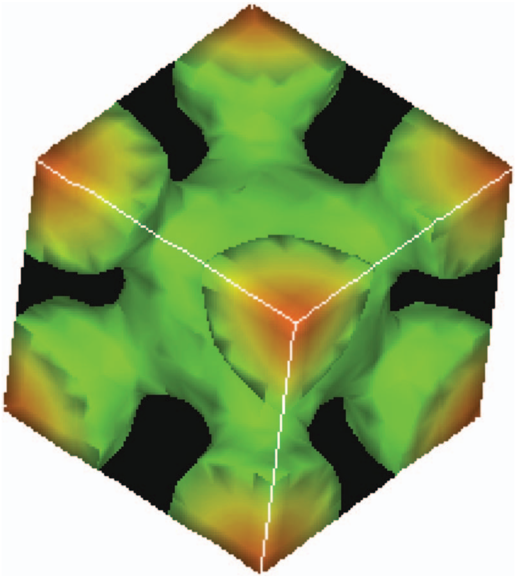

FIG. 5. (Color) Three-dimensional isosurface of the occupation number density of β-PdH$_{0.84}$. The value at the surface is 0.60 electron/a.u.^{3}.

The authors thank Y. Tanaka for helpful discussion on the reconstruction procedure of electron momentum distribution. The computational code of FLAPW calculation including Compton profile calculation was developed by Kodama, Hamada, and Yanase. The Compton scattering experiment was performed with the approval of JASRI (Grant No. 2003A0329-ND3-np). This work was partially supported by Grant-in-Aid for Scientific Research (Grant No. 14350041) from MEXT of Japan.

---

*Electronic address: smizusaki@ee.aoyama.ac.jp

[1] B. Stritzker and W. Buckel, Z. Phys. **257**, 1 (1972).
[2] A. C. Switendick, Ber. Bunsenges. Phys. Chem. **76**, 535 (1972).
[3] D. A. Papaconstantopoulos, B. M. Klein, E. N. Economou, and L. L. Boyer, Phys. Rev. B **17**, 141 (1978).
[4] D. A. Papaconstantopoulos, B. M. Klein, J. S. Faulkner, and L. L. Boyer, Phys. Rev. B **18**, 2784 (1978).
[5] C. T. Chan and S. G. Louie, Phys. Rev. B **27**, 3325 (1983).
[6] A. Harmalkar, D. G. Kanhere, and R. M. Singru, Phys. Rev. B **31**, 6415 (1985).
[7] M. Gupta and A. J. Freeman, Phys. Rev. B **17**, 3029 (1978).
[8] S. Tewari and R. M. Singru, Solid State Commun. **36**, 721 (1980).
[9] D. E. Eastman, J. K. Cashion, and A. C. Switendick, Phys. Rev. Lett. **27**, 35 (1971).
[10] M. Gupta and L. Schlapbach, in *Hydrogen in Intermetallic Compounds I*, edited by L. Schlapbach (Springer, Berlin, 1988), p. 139.
[11] P. A. Bennett and J. C. Fuggle, Phys. Rev. B **26**, 6030 (1982).
[12] A. Kshirsagar, D. G. Kanhere, and R. M. Singru, Phys. Rev. B **34**, 853 (1986).
[13] S. Sinha, S. Badrinarayanan, and A. P. B. Sinha, J. Phys. F: Met. Phys. **16**, L229 (1986).
[14] M. Hasegawa, H. Asano, and M. Hirabayashi, in *Positron Annihilation*, edited by P. G. Coleman, S. C. Sharma, and L. M. Diana (North-Holland, Amsterdam, 1982), p. 234.
[15] H. L. M. Bakker, R. Griessen, N. J. Koeman, P. Albers, and G. H. Sicking, J. Phys. F: Met. Phys. **16**, 721 (1986).
[16] R. Griessen and L. M. Huisman, in *Electronic Structure and Properties of Hydrogen in Metals*, edited by P. Jena and C. B. Satterthwaite (Plenum Press, New York, 1983), p. 235.
[17] Y. Tanaka, N. Sakai, Y. Kubo, and H. Kawata, Phys. Rev. Lett. **70**, 1537 (1993).
[18] G. Stutz, F. Wohlert, A. Kaprolat, W. Shülke, Y. Sakurai, Y. Tanaka, M. Ito, H. Kawata, N. Shiotani, S. Kaprzyk, and A. Bansil, Phys. Rev. B **60**, 7099 (1999).
[19] Y. Tanaka, Y. Sakurai, A. T. Stewart, N. Shiotani, P. E. Mijnarends, S. Kaprzyk, and A. Bansil, Phys. Rev. B **63**, 45120 (2001).
[20] I. Matsumoto, J. Kwiatkowska, F. Maniawski, M. Itou, H. Kawata, N. Shiotani, S. Kaprzyk, P. E. Mijnarends, B. Barbiellini, and A. Bansil, Phys. Rev. B **64**, 45121 (2001).
[21] I. Matsumoto, H. Kawata, and N. Shiotani, Phys. Rev. B **64**, 195132 (2001).
[22] G. Kontrym-Sznajd, M. Samsel-Czekala, A. Pietrazsko, H. Sormann, S. Manninen, S. Huotari, K. Hämäläinen, J. Laukkanen, R. N. West, and W. Schülke, Phys. Rev. B **66**, 155110 (2002).
[23] G. Kontrym-Sznajd, M. Samsel-Czekala, S. Huotari, K. Hämäläinen, and S. Manninen, Phys. Rev. B **68**, 155106 (2003).
[24] M. Samsel-Czakala, G. Kontrym-Sznajd, G. Doring, W. Schulke, J. Kwiatkowska, F. Maniawski, S. Kaprzyk, and A. Bansil, Appl. Phys. A: Mater. Sci. Process. **87**, 76 (2003).
[25] Y. Sakurai, Y. Tanaka, A. Bansil, S. Kaprzyk, A. T. Stewart, Y. Nagashima, T. Hyodo, S. Nanao, H. Kawata, and N. Shiotani, Phys. Rev. Lett. **74**, 2252 (1995).
[26] A consistent Fermi surface has been obtained by the first derivatives of the electron occupation density (EOD). In this work, however, we employed the first derivatives of the electron momentum density (EMD) for the experimental determination of the Fermi surface since those of EMD show extrema with narrower peaks than those of EOD.
[27] S. Mizusaki, N. Hiraoka, I. Yamamoto, M. Itou, Y. Sakurai, and M. Yamaguchi, J. Phys. Soc. Jpn. **72**, 1145 (2003).
[28] R. Suzuki, M. Osawa, S. Tanigawa, M. Matsumoto, and N. Shiotani, J. Phys. Soc. Jpn. **58**, 3251 (1989).
[29] D. G. Lock, V. H. C. Crisp, and R. N. West, J. Phys. F: Met. Phys. **3**, 561 (1973).
[30] H. V. Bohm and V. J. Esterling, Phys. Rev. **128**, 1021 (1962).